Colloquia: Channeling 2010

Coherent X-radiation of a relativistic electron on nano-scale multilayer structure in Laue scattering geometry

S. Blazhevich([1]) and A. Noskov([2])

([1]) *Belgorod State University - Belgorod, Russia*
([2]) *Belgorod University of Consumer's Cooperation - Belgorod, Russia*

Summary. — The coherent X-radiation of relativistic electron crossing a periodic multilayer artificial structure is considered in Laue geometry. The expressions describing spectral-angular characteristics of the radiation are derived. The possibility of the radiation photon yield material increase with change of the asymmetry of the relativistic electron Coulomb field reflection with respect to multilayer target entrance surface is considered.

PACS `41.60.-m` – Radiation by moving charges.
PACS `41.75.Ht` – Relativistic electron and positron beams.
PACS `42.25.Fx` – Diffraction and scattering.

1. – Introduction

Traditionally the relativistic particle radiation in a periodic lamellar structure would be considered in Bragg scattering geometry, when the reflecting layers are situated parallel to the entrance surface, that is in symmetric case. The radiation would be considered as resonance transition radiation [1,2]. Some progress has been made recently in the description of the radiation in such media [3], where the radiation in a multilayer periodic medium is represented as the sum of diffraction transition radiation (DTR) and parametric X-radiation (PXR) by analogy with the relativistic electron coherent radiation in single-crystal media [4-7].

In the present work the coherent X-radiation in artificial periodic structure is considered for the first time in Laue scattering geometry under arbitrary asymmetry of the relativistic electron Coulomb field reflection with respect to the target surface by analogy with the radiation in a single crystal. In this geometry surface as opposed to the traditional symmetric case of Bragg reflection geometry [1-3] the emitted photons leave the target through its back surface and for the photons of high frequency their wave vectors form wide angles with the target. The expression of the radiation spectral-angular density is obtained based on dynamic diffraction theory two-wave approximation. It is shown that practically in the same conditions the yield of photons from a periodical
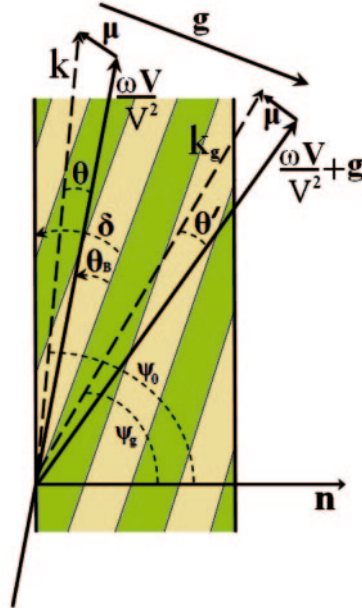
Fig. 1. – Scheme of the radiation process of relativistic electron in multilayer structure (k and k_g are incident and diffracted pseudophotons).

lamellar structure is an order of magnitude greater than that from a crystal medium. The opportunity is also shown of increasing the spectral-angular density and integral yield of photons by change of asymmetry of the relativistic electron Coulomb field reflection with respect to the multilayer target entrance surface.

The result derived can be used as the principal basis for creating an alternative quasi-monochromatic X-ray source with varying photon frequency.

2. – Radiation amplitude

Let us consider the radiation of a fast charged particle crossing a multilayer periodic structure with steady speed $\mathbf{V}$ (see in fig. 1) consisting of periodically situated amorphous layers of thicknesses a and b ($T = a + b$ is the structure period) having the dielectric susceptibility χ_a and χ_b, respectively.

Let us consider the equation for Fourier transform of electromagnetic field

$$(1) \qquad \mathbf{E}(\mathbf{k}, \omega) = \int \mathrm{d}t \, \mathrm{d}^3 \mathbf{r} \, \mathbf{E}(\mathbf{r}, t) \exp\left[i\omega t - i\mathbf{k}\mathbf{r}\right].$$

Since the field of a relativistic particle could, to a good accuracy, be taken as being transverse, the incident $\mathbf{E}_0(\mathbf{k}, \omega)$ and diffracted $\mathbf{E_g}(\mathbf{k}, \omega)$ electromagnetic waves are determined by two amplitudes with different values of transverse polarization:

$$(2) \qquad \begin{aligned} \mathbf{E}_0(\mathbf{k}, \omega) &= E_0^{(1)}(\mathbf{k}, \omega)\mathbf{e}_0^{(1)} + E_0^{(2)}(\mathbf{k}, \omega)\mathbf{e}_0^{(2)}, \\ \mathbf{E_g}(\mathbf{k}, \omega) &= E_{\mathbf{g}}^{(1)}(\mathbf{k}, \omega)\mathbf{e}_1^{(1)} + E_{\mathbf{g}}^{(2)}(\mathbf{k}, \omega)\mathbf{e}_1^{(2)}. \end{aligned}$$

The unit vectors of polarization $\mathbf{e}_0^{(1)}$, $\mathbf{e}_0^{(2)}$, $\mathbf{e}_1^{(1)}$ and $\mathbf{e}_1^{(2)}$ are chosen in the following way. Vectors $\mathbf{e}_0^{(1)}$ and $\mathbf{e}_0^{(2)}$ are perpendicular to vector $\mathbf{k}$, and vectors $\mathbf{e}_1^{(1)}$ and $\mathbf{e}_1^{(2)}$ are perpendicular to vector $\mathbf{k_g} = \mathbf{k} + \mathbf{g}$. Vectors $\mathbf{e}_0^{(2)}$, $\mathbf{e}_1^{(2)}$ are situated on the plane of vectors $\mathbf{k}$ and $\mathbf{k_g}$ (π-polarization) and $\mathbf{e}_0^{(1)}$, $\mathbf{e}_1^{(1)}$ are perpendicular to this plane (σ-polarization); $\mathbf{g}$ is analogous to the vector of the reciprocal lattice, it is perpendicular to the layers and has module $g = \frac{2\pi}{T} n$, $n = 0, \pm 1, \pm 2, \ldots$.

The system of equations for the Fourier transform images of electromagnetic field in two-wave approximation of diffraction dynamic theory has the following form [8]:

$$(3) \quad \begin{cases} (\omega^2(1 + \chi_0) - k^2)E_0^{(s)} + \omega^2 \chi_{-\mathbf{g}} C^{(s,\tau)} E_\mathbf{g}^{(s)} = 8\pi^2 i e \omega \theta V P^{(s)} \delta(\omega - \mathbf{kV}), \\ \omega^2 \chi_\mathbf{g} C^{(s,\tau)} E_0^{(s)} + (\omega^2(1 + \chi_0) - k_\mathbf{g}^2)E_\mathbf{g}^{(s)} = 0, \end{cases}$$

where $\chi_0 = \chi_0' + i\chi_0''$ is the average dielectric susceptibility, $\chi_\mathbf{g}$, $\chi_{-\mathbf{g}}$ are the coefficients of the Fourier expansion of the dielectric susceptibility of a crystal over the reciprocal lattice vectors $\mathbf{g}$.

$$(4) \qquad \chi(\omega, \mathbf{r}) = \sum_\mathbf{g} \chi_\mathbf{g}(\omega) \exp[i\mathbf{gr}] = \sum_\mathbf{g} \left(\chi_\mathbf{g}'(\omega) + i\chi_\mathbf{g}''(\omega) \right) \exp[i\mathbf{gr}].$$

The values $\tilde{N}^{(s)}$ and $P^{(s)}$ are defined in the system (3) as

$$(5) \qquad C^{(s)} = \mathbf{e}_0^{(s)} \mathbf{e}_1^{(s)}, \qquad \tilde{N}^{(1)} = 1, \qquad \tilde{N}^{(2)} = \cos 2\theta_B,$$
$$P^{(s)} = \mathbf{e}_0^{(s)}(\boldsymbol{\mu}/\mu), \qquad P^{(1)} = \sin\varphi, \qquad P^{(2)} = \cos\varphi,$$

where $\boldsymbol{\mu} = \mathbf{k} - \omega\mathbf{V}/V^2$ is the virtual photon momentum vector component perpendicular to the particle velocity vector $\mathbf{V}$ ($\mu = \omega\theta/V$, where $\theta \ll 1$ is the angle between vectors $\mathbf{k}$ and $\mathbf{V}$), θ_B is the angle between electron velocity and a set of atomic planes in the crystal (Bragg angle), φ is the azimuth angle, counted off from the plane formed by vectors $\mathbf{V}$ and $\mathbf{g}$, the value of the reciprocal lattice vector is shown by the expression $g = 2\omega_B \sin\theta_B/V$, ω_B is Bragg's frequency. The angle between vector $\frac{\omega\mathbf{V}}{V^2} + \mathbf{g}$ and diffracted wave vector $\mathbf{k_g}$ is defined as θ'. The equation system (3) under $s = 1$ describes the fields of σ-polarization, and under $s = 2$ the fields of π-polarization.

It is not too difficult to show that the magnitudes of the Fourier coefficients χ_0 and $\chi_\mathbf{g}$ have such a form:

$$(6) \qquad \chi_0(\omega) = (a\chi_a + b\chi_b)/T, \qquad \chi_\mathbf{g}(\omega) = (\exp[-iga] - 1)(\chi_b - \chi_a)/igT,$$

where $g = 2\pi n/T$, $n = 0, \pm 1, \pm 2, \ldots$.

The relation

$$(7) \qquad \begin{aligned} \chi_0' &= (a\chi_a' + b\chi_b')/T, \\ \chi_0'' &= (a\chi_a'' + b\chi_b'')/T, \\ \mathrm{Re}\,\sqrt{\chi_\mathbf{g}\chi_{-\mathbf{g}}} &= 2\sin(ga/2)(\chi_b' - \chi_a')/gT, \\ \mathrm{Im}\,\sqrt{\chi_\mathbf{g}\chi_{-\mathbf{g}}} &= 2\sin(ga/2)(\chi_b'' - \chi_a'')/gT \end{aligned}$$

following from (6) will be used further.

When solving the dispersion equation following from (3)

$$(8) \qquad (\omega^2(1+\chi_0) - k^2)(\omega^2(1+\chi_0) - k_{\mathbf{g}}^2) - \omega^4 \chi_{-\mathbf{g}} \chi_{\mathbf{g}} C^{(s)^2} = 0$$

by a standard method of dynamic theory [9], we will find expressions for k and $k_{\mathbf{g}}$:

$$(9) \qquad k = \omega\sqrt{1+\chi_0} + \lambda_0, \qquad k_{\mathbf{g}} = \omega\sqrt{1+\chi_0} + \lambda_{\mathbf{g}},$$

$$(10) \qquad \lambda_{\mathbf{g}}^{(1,2)} = \frac{\omega}{4}\left(\beta \pm \sqrt{\beta^2 + 4\chi_{\mathbf{g}}\chi_{-\mathbf{g}}C^{(s)2}\frac{\gamma_{\mathbf{g}}}{\gamma_0}}\right),$$

$$\lambda_0^{(1,2)} = \omega\frac{\gamma_0}{4\gamma_{\mathbf{g}}}\left(-\beta \pm \sqrt{\beta^2 + 4\chi_{\mathbf{g}}\chi_{-\mathbf{g}}C^{(s)2}\frac{\gamma_{\mathbf{g}}}{\gamma_0}}\right),$$

where $\beta = \alpha - \chi_0(1 - \gamma_{\mathbf{g}}/\gamma_0)$, $\alpha = (k_g^2 - k^2)/\omega^2$, $\gamma_0 = \cos\psi_0$, $\gamma_{\mathbf{g}} = \cos\psi_{\mathbf{g}}$, ψ_0 —the angle between the wave vector of the incident wave $\mathbf{k}$ and the vector of the normal to the plate surface $\mathbf{n}$, $\psi_{\mathbf{g}}$— the angle between the wave vector $\mathbf{k}_{\mathbf{g}}$ and the vector $\mathbf{n}$ (see fig. 1).

The dynamic addition agents λ_0 and $\lambda_{\mathbf{g}}$ for the X-ray waves are bound by the relation $\lambda_{\mathbf{g}} = \omega\beta/2 + \lambda_0(\gamma_{\mathbf{g}}/\gamma_0)$. As for $|\lambda_0| \ll \omega$ and $|\lambda_{\mathbf{g}}| \ll \omega$, it can be proved that $\theta \approx \theta'$ (see fig. 1), therefore we will use symbol θ on all occasions.

The solution of the combined equations (3) gives us the relativistic particle diffracted field inside the periodic structure as

$$(11a) \qquad E_{\mathbf{g}}^{(s)\mathrm{cr}} = -\frac{8\pi^2 ieV\theta P^{(s)}}{\omega}\frac{\omega^2\chi_{\mathbf{g}}C^{(s)}}{4\frac{\gamma_0^2}{\gamma_{\mathbf{g}}^2}\left(\lambda_{\mathbf{g}} - \lambda_{\mathbf{g}}^{(1)}\right)\left(\lambda_{\mathbf{g}} - \lambda_{\mathbf{g}}^{(2)}\right)}\delta\left(\lambda_{\mathbf{g}} - \lambda_{\mathbf{g}}^*\right)$$

$$+E_{\mathbf{g}}^{(s)^{(1)}}\delta\left(\lambda_{\mathbf{g}} - \lambda_{\mathbf{g}}^{(1)}\right) + E_{\mathbf{g}}^{(s)^{(1)}}\delta\left(\lambda_{\mathbf{g}} - \lambda_{\mathbf{g}}^{(2)}\right),$$

where $\lambda_0^* = \omega(\gamma^{-2} + \theta^2 - \chi_0)/2$, $\lambda_{\mathbf{g}}^* = \omega\beta/2 + (\gamma_{\mathbf{g}}/\gamma_0)\lambda_0^*$, $\gamma = 1/\sqrt{1 - V^2}$ —the particle Lorentz factor, $E_{\mathbf{g}}^{(s)^{(1)}}$ and $E_{\mathbf{g}}^{(s)^{(1)}}$ —the free diffracted fields in multilayer target.

The same field in the vacuum in front of the target is given as

$$(11b) \qquad E_0^{(s)\mathrm{vac\,I}} = \frac{8\pi^2 ieV\theta P^{(s)}}{\omega}\frac{\gamma_{\mathbf{g}}}{\gamma_0}\left(-\chi_0 - \frac{2}{\omega}\frac{\gamma_0}{\gamma_{\mathbf{g}}}\lambda_{\mathbf{g}} + \beta\frac{\gamma_0}{\gamma_{\mathbf{g}}}\right)^{-1}\delta\left(\lambda_{\mathbf{g}} - \lambda_{\mathbf{g}}^*\right).$$

Here the relation $\delta(\lambda_0 - \lambda_0^*) = \frac{\gamma_{\mathbf{g}}}{\gamma_0}\delta(\lambda_{\mathbf{g}} - \lambda_{\mathbf{g}}^*)$ is used. The field in the vacuum behind the multilayer target is given as $E_{\mathbf{g}}^{(s)\mathrm{vac}} = E_{\mathbf{g}}^{(s)\mathrm{Rad}}\delta(\lambda_{\mathbf{g}} + \omega\chi_0/2)$, where $E_{\mathbf{g}}^{(s)\mathrm{Rad}}$ is the field of coherent radiation near Bragg direction.

The following expression bounding the diffracted and incident fields inside of the multilayer structure results from the second equation of system (3):

$$(12) \qquad E_0^{(s)\mathrm{cr}} = 2\omega\lambda_{\mathbf{g}}\left(\omega^2\chi_g C^{(s)}\right)^{-1}E_{\mathbf{g}}^{(s)\mathrm{cr}}.$$

For definition of amplitude $E_{\mathbf{g}}^{(s)\mathrm{Rad}}$ we will use the ordinary boundary conditions on the inlet and outlet surfaces of the multilayer plate:

(13)
$$\int E_0^{(s)\mathrm{vac\,I}}\mathrm{d}\lambda_0 = \int E_0^{(s)\mathrm{cr}}\mathrm{d}\lambda_0, \qquad \int E_{\mathbf{g}}^{(s)\mathrm{cr}}\mathrm{d}\lambda_0 = 0,$$

$$\int E_{\mathbf{g}}^{(s)\mathrm{cr}} \exp\left[i\frac{\lambda_{\mathbf{g}}}{\gamma_{\mathbf{g}}}L\right]\mathrm{d}\lambda_{\mathbf{g}} = \int E_{\mathbf{g}}^{(s)\mathrm{vac}} \exp\left[i\frac{\lambda_{\mathbf{g}}}{\gamma_{\mathbf{g}}}L\right]\mathrm{d}\lambda_{\mathbf{g}}.$$

Hence we will obtain the expression for the radiation field:

(14)
$$E_{\mathbf{g}}^{(s)\mathrm{Rad}} = \frac{8\pi^2 ieV\theta P^{(s)}}{\omega}\frac{\omega^2\chi_{\mathbf{g}}C^{(s)}\exp\left[i\left(\frac{\omega\chi_0}{2}+\lambda_g^*\right)\frac{L}{\gamma_g}\right]}{2\omega\frac{\gamma_0}{\gamma_{\mathbf{g}}}\left(\lambda_{\mathbf{g}}^{(1)}-\lambda_{\mathbf{g}}^{(2)}\right)}$$

$$\times\left[\left(\frac{\omega}{-\chi_0\omega-2\lambda_0^*}+\frac{\omega}{2\frac{\gamma_0}{\gamma_{\mathbf{g}}}(\lambda_{\mathbf{g}}^*-\lambda_{\mathbf{g}}^{(2)})}\right)\times\right.$$

$$\times\left(1-\exp\left[-i\frac{\lambda_{\mathbf{g}}^*-\lambda_{\mathbf{g}}^{(2)}}{\gamma_{\mathbf{g}}}L\right]\right)-\left(\frac{\omega}{-\chi_0\omega-2\lambda_0^*}+\frac{\omega}{2\frac{\gamma_0}{\gamma_{\mathbf{g}}}(\lambda_{\mathbf{g}}^*-\lambda_{\mathbf{g}}^{(1)})}\right)$$

$$\left.\times\left(1-\exp\left[-i\frac{\lambda_{\mathbf{g}}^*-\lambda_{\mathbf{g}}^{(1)}}{\gamma_{\mathbf{g}}}L\right]\right)\right].$$

The terms in square brackets in (14) correspond to two branches of solution for X-ray waves excited in the multilayer structure.

For further analysis of the radiation let us present the dynamic addition agent (10) as

(15) $\lambda_g^{(1,2)} = \dfrac{\omega|\chi_{\mathbf{g}}'|C^{(s)}}{2}\left(\xi^{(s)} - \dfrac{i\rho^{(s)}(1-\varepsilon)}{2}\right.$

$$\left.\pm\sqrt{\xi^{(s)2}+\varepsilon-2i\rho^{(s)}\left(\frac{(1-\varepsilon)}{2}\xi^{(s)}+\kappa^{(s)}\varepsilon\right)-\rho^{(s)2}\left(\frac{(1-\varepsilon)^2}{4}+\kappa^{(s)2}\varepsilon\right)}\right),$$

where

(16) $\xi^{(s)}(\omega) = \eta^{(s)}(\omega) + \dfrac{1-\varepsilon}{2\nu^{(s)}}, \qquad \eta^{(s)}(\omega) = \dfrac{\sin^2\theta_B gT}{V^2 C^{(s)}|\chi_b'-\chi_a'|\left|\sin\left(\frac{ga}{2}\right)\right|}$

$$\times\left(1-\frac{\omega(1-\theta\cos\varphi\cot\theta_B)}{\omega_B}\right),$$

$$\nu^{(s)} = \frac{2C^{(s)}\sin\left(\frac{ga}{2}\right)}{g}\frac{\chi_b'-\chi_a'}{a\chi_a'+b\chi_b'}, \qquad \rho^{(s)} = \frac{a\chi_a''+b\chi_b''}{|\chi_b'-\chi_a'|C^{(s)}}\frac{g}{2\left|\sin\left(\frac{ga}{2}\right)\right|},$$

$$\kappa^{(s)} = \frac{2C^{(s)}\sin\left(\frac{ga}{2}\right)}{g}\frac{\chi_b''-\chi_a''}{a\chi_a''+b\chi_b''}, \qquad \varepsilon = \frac{\gamma_{\mathbf{g}}}{\gamma_0}.$$
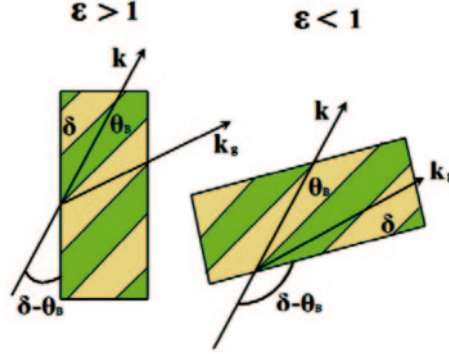
Fig. 2. – Radiation process under different reflection asymmetry.

An important parameter in expression (16), parameter ε, can be expressed by the formula

$$(17) \qquad \varepsilon = \sin(\delta + \theta_B)/\sin(\delta - \theta_B)$$

that defines the degree of the field reflection asymmetry with respect to the multilayer target entrance surface. Here θ_B is the angle between electron velocity and reflecting layers, δ is the angle between target surface and the reflecting layers. Let us note that the angle of the electron incidence with respect to the multilayer target surface $\delta - \theta_B$ increases if the parameter ε decreases and the opposite (see fig. 2). In the case of symmetric reflection the incident and diffracted photon vectors make equal angles with respect to the target surface (see fig. 2), but in the case of asymmetric reflection these angles are different. In the symmetric case $\varepsilon = 1$ and $\delta = \pi/2$, in the asymmetric one $\varepsilon \neq 1$ and $\delta \neq \pi/2$.

3. – Radiation spectral-angular distribution

Substituting (14) for the well-known [8] expression for spectral-angular density of X-radiation

$$(18) \qquad \omega \frac{\mathrm{d}^2 N}{\mathrm{d}\omega \mathrm{d}\Omega} = \omega^2 (2\pi)^{-6} \sum_{s=1}^{2} \left| E_{\mathbf{g}}^{(s)\mathrm{Rad}} \right|^2, \qquad E_{\mathbf{g}}^{(s)\mathrm{Rad}} = E_{\mathrm{PXR}}^{(s)} + E_{\mathrm{DTR}}^{(s)},$$

we will find the expressions describing the PXR and DTR contributions to total spectral-angular density of the radiation and the summand being the result of these radiation mechanisms interference:

$$(19a) \qquad \omega \frac{\mathrm{d}^2 N_{\mathrm{PXR}}^{(s)}}{\mathrm{d}\omega \mathrm{d}\Omega} = \frac{e^2}{4\pi^2} P^{(s)2} \frac{\theta^2}{(\theta^2 + \gamma^{-2} - \chi_0')^2} R_{\mathrm{PXR}}^{(s)},$$

$$(19b) \qquad R_{\mathrm{PXR}}^{(s)} = \left(1 - \xi/\sqrt{\xi^2 + \varepsilon}\right)^2$$

$$\times \frac{1 + \exp\left[-2b^{(s)}\rho^{(s)}\Delta^{(1)}\right] - 2\exp\left[-b^{(s)}\rho^{(s)}\Delta^{(1)}\right]\cos(b^{(s)}\Delta(\omega))}{\Delta(\omega)^2 + \rho^{(s)2}\Delta^{(1)2}},$$

(20a) $\omega \dfrac{\mathrm{d}^2 N_{\mathrm{DTR}}^{(s)}}{\mathrm{d}\omega\mathrm{d}\Omega} = \dfrac{e^2}{4\pi^2} P^{(s)2} \theta^2 \left(\dfrac{1}{\theta^2 + \gamma^{-2}} - \dfrac{1}{\theta^2 + \gamma^{-2} - \chi_0'} \right)^2 R_{\mathrm{DTR}}^{(s)},$

(20b) $\quad R_{\mathrm{DTR}}^{(s)} = \dfrac{4\varepsilon^2}{\xi^2 + \varepsilon} \exp\left[-b^{(s)} \rho^{(s)} \dfrac{1+\varepsilon}{\varepsilon} \right] \times$

$$\times \left[\sin^2\left(b^{(s)} \dfrac{\left(\sqrt{\xi^2 + \varepsilon}\right)}{\varepsilon} \right) + sh^2\left(b^{(s)} \rho^{(s)} \dfrac{(1-\varepsilon)\xi^{(s)} + 2\varepsilon\kappa^{(s)}}{2\varepsilon\sqrt{\xi^2 + \varepsilon}} \right) \right],$$

(21a) $\omega \dfrac{\mathrm{d}^2 N_{\mathrm{INT}}^{(s)}}{\mathrm{d}\omega\mathrm{d}\Omega} = \dfrac{e^2}{4\pi^2} P^{(s)2} \theta^2 \left(\dfrac{1}{\theta^2 + \gamma^{-2}} - \dfrac{1}{\theta^2 + \gamma^{-2} - \chi_0'} \right) \dfrac{1}{\theta^2 + \gamma^{-2} - \chi_0'} R_{\mathrm{INT}}^{(s)},$

(21b) $\quad R_{\mathrm{INT}}^{(s)} = -\dfrac{2\varepsilon}{\xi^{(s)2} + \varepsilon} \operatorname{Re}\left(\left(\xi^{(s)} - \sqrt{\xi^{(s)2} + \varepsilon} \right) \right.$

$$\times \dfrac{1 - \exp\left[-ib^{(s)}\Delta(\omega) - b^{(s)}\rho^{(s)}\Delta^{(1)} \right]}{\Delta(\omega) - i\rho^{(s)}\Delta^{(1)}} \times$$

$$\left. \times \left(\exp\left[ib^{(s)}\Delta(\omega) - b^{(s)}\rho^{(s)}\Delta^{(1)} \right] - \exp\left[ib^{(s)}\Delta(\omega) - b^{(s)}\rho^{(s)}\Delta^{(2)} \right] \right) \right),$$

where

(22) $\quad \Delta(\omega) = \sigma^{(s)} + \left(\xi(\omega) - \sqrt{\xi(\omega)^2 + \varepsilon} \right) \Big/ \varepsilon,$

$$\Delta^{(2)} = \dfrac{\varepsilon + 1}{2\varepsilon} + \dfrac{1 - \varepsilon}{2\varepsilon} \dfrac{\xi^{(s)}}{\sqrt{\xi^{(s)2} + \varepsilon}} + \dfrac{\kappa^{(s)}}{\sqrt{\xi^{(s)2} + \varepsilon}},$$

$$\Delta^{(1)} = \dfrac{\varepsilon + 1}{2\varepsilon} - \dfrac{1 - \varepsilon}{2\varepsilon} \dfrac{\xi^{(s)}}{\sqrt{\xi^{(s)2} + \varepsilon}} - \dfrac{\kappa^{(s)}}{\sqrt{\xi^{(s)2} + \varepsilon}}, \qquad \sigma^{(s)} = \dfrac{1}{\nu^{(s)}}(\mathbf{P}(\theta, \gamma) + 1),$$

$$\mathbf{P}(\theta, \gamma) = \theta^2 / |\chi_0'| + \gamma^{-2} / |\chi_0'|, \qquad b^{(s)} = \dfrac{\omega \left| \operatorname{Re} \sqrt{\chi_{\mathbf{g}}\chi_{-\mathbf{g}}} \right| C^{(s)}}{2} \dfrac{L}{\gamma_0}.$$

The solution of the corresponding equation $\Delta(\omega) = 0$ (see (19b)) defines the frequency ω_*, in the vicinity of which the spectrum of the PXR photons radiated under fixed radiation (observation) angle is concentrated.

4. – Radiation angular density

By integrating (19)–(21) over frequency function $\eta^{(s)}(\omega)$ we will obtain the expressions for angular densities of these radiations:

(23) $\qquad \dfrac{\mathrm{d}N_{\mathrm{PXR}}^{(s)}}{\mathrm{d}\Omega} = \dfrac{e^2 P^{(s)2} \nu^{(s)}}{8\pi^2 \sin^2\theta_B} \dfrac{\theta^2/|\chi_0'|}{(\mathbf{P}(\theta, \gamma) + 1)^2} \int_{-\infty}^{+\infty} R_{\mathrm{PXR}}^{(s)} \mathrm{d}\eta^{(s)}(\omega),$

(24) $\qquad \dfrac{\mathrm{d}N_{\mathrm{DTR}}^{(s)}}{\mathrm{d}\Omega} = \dfrac{e^2 P^{(s)2} \nu^{(s)}}{8\pi^2 \sin^2\theta_B} \dfrac{\theta^2/|\chi_0'|}{(\mathbf{P}(\theta, \gamma) + 1)^2 \mathbf{P}(\theta, \gamma)^2} \int_{-\infty}^{+\infty} R_{\mathrm{DTR}}^{(s)} \mathrm{d}\eta^{(s)}(\omega),$

(25) $\qquad \dfrac{\mathrm{d}N_{\mathrm{INT}}^{(s)}}{\mathrm{d}\Omega} = \dfrac{e^2 P^{(s)2} \nu^{(s)}}{8\pi^2 \sin^2\theta_B} \dfrac{\theta^2/|\chi_0'|}{(\mathbf{P}(\theta, \gamma) + 1)^2 \mathbf{P}(\theta, \gamma)} \int_{-\infty}^{+\infty} R_{\mathrm{INT}}^{(s)} \mathrm{d}\eta^{(s)}(\omega),$

where $\mathbf{P}(\theta, \gamma) = \theta^2 / |\chi_0'| + \gamma^{-2} / |\chi_0'|$.
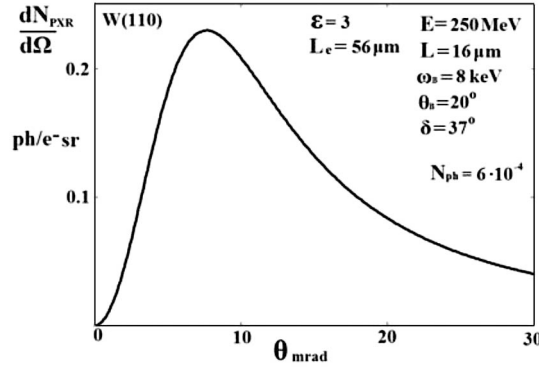
Fig. 3.

5. – Analyses of the process of the relativistic electron radiation in artificial structures

As was noted above, the photon reflections from artificial multilayer periodic structure are usually considered in Bragg scattering geometry only in the case of symmetric reflection, though in single crystal the radiation is investigated basically in Laue geometry.

Expressions (19)-(21) and (23)-(25) represent the main results in the present work. These expressions are obtained based on two-wave approximation of dynamic theory of diffraction and allow the investigation of the spectral-angular characteristics of the coherent radiation of the charged relativistic particles in artificial periodic structures taking into account well-known dynamic effects in physics of scattering of free X-radiation photon in crystal [9] and predicted recently by the authors of the article for pseudophotons of the relativistic electron Coulomb field [10-12]. Particularly, these expressions allow to investigate the dependences of radiation characteristics on parameters of amorphous layers a and b, on the material parameters χ_a and χ_b, on the parameter of reflection symmetry $\varepsilon(\delta, \theta_B)$ (look in (17)) and so on.

The calculations were carried out for spectral-angular distributions of the radiation generated by relativistic electrons under different values of parameters of multilayer periodic structure and incident particle energy.

The curves of the angular density distributions of the relativistic electron PXR ($\omega_B = 8\,\text{keV}$) calculated for analogues conditions for tungsten W single-crystal target and periodic multilayer structure of amorphous layers of W and Be are represented in fig. 3 and fig. 4. For both the targets the same length of the electron path $L_e = 56\,\mu\text{m}$ and the same value of reflection asymmetry $\varepsilon = 3$ were taken in the calculations. As follows from figs. 3 and 4 the angular density of PXR from multilayer structure exceeds 20 times the angular density of the radiation from a single-crystal target.

The total yield of the PXR photons from a multilayer structure at this case exceeds 15 times the total yield of photons from a single-crystal target. This effect is caused by the considerable widening of radiation spectrum formed in the multilayer structure (figs. 5, 6) because the electron crosses a less number of heterogeneities in this target. The curves describing the PXR spectrum are calculated by formula (19b).

The PXR photon yield can also be increased by the reflection asymmetry increase, *i.e.* by the change of parameter ε (see fig. 7), herewith the increase of the angular density is connected with the widening of PXR spectral peak like for a single-crystal target [11].
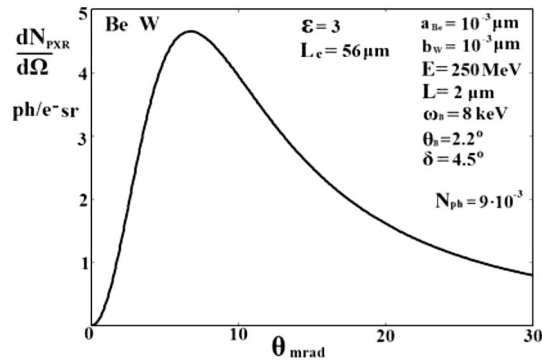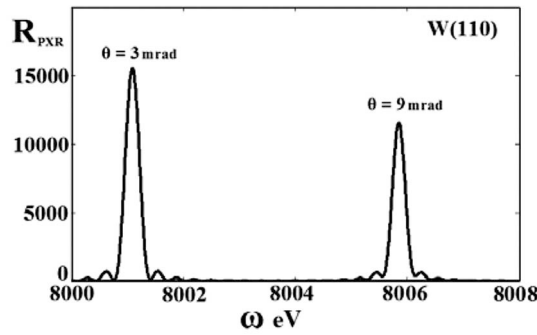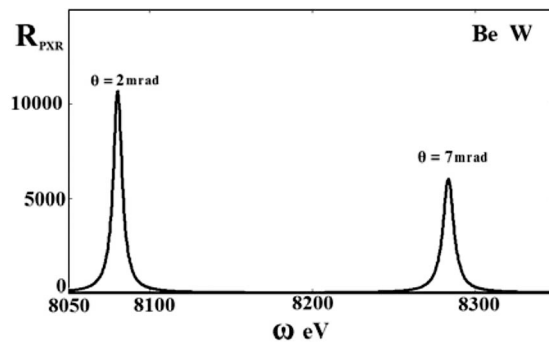
Fig. 4.

Fig. 5.

Fig. 6.

In figs. 8–10 the curves of angular density of the radiation ($\omega_B = 250\,\text{åV}$) are given for the case when the relativistic electron crosses the multilayer Be-Mo (beryllium-molybdenum) target.

In fig. 8 the curves of angular density PXR demonstrate the considerable yield of X-radiation photons with energy which is appropriate for medicinal goals.
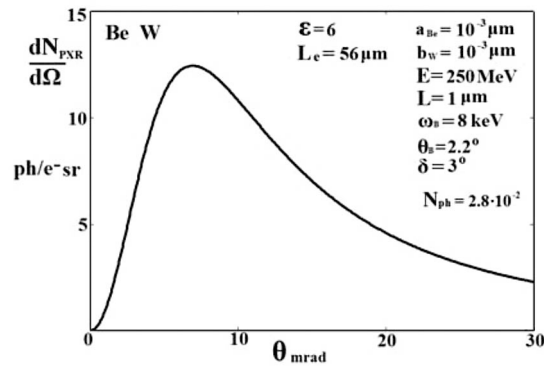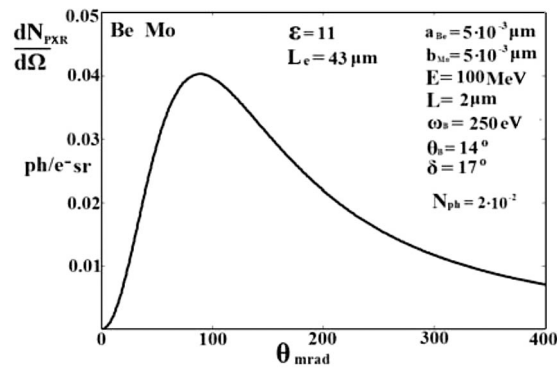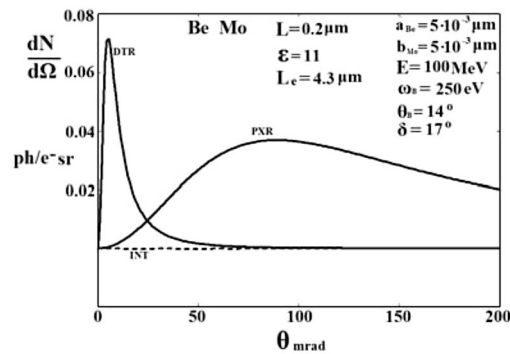
Fig. 7.

Fig. 8.

Fig. 9.

In fig. 9 the curves of angular density of DTR and PXR demonstrate the yield of photons from a thin target (under weak absorption of the radiation). One can see that the contribution of diffracted transition radiation originated on the inlet surface of the target is considerable in this case. It is seen from fig. 8 and fig. 9 that PXR photon yield becomes saturated for "thick" target (fig. 8).
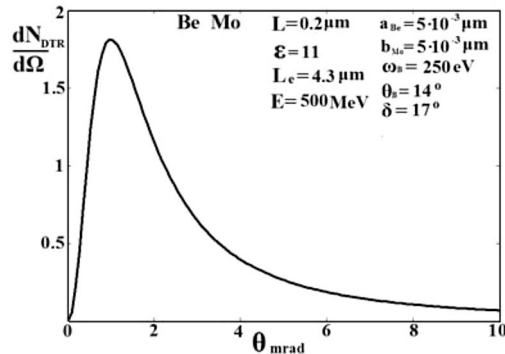
Fig. 10.

Figure 10 demonstrates the increase of the DTR contribution to the total yield when the incident electron energy increases and becomes the main. It is necessary to note that DTR is more directed in comparison with PXR.

6. – Conclusion

A theory of coherent radiation of the relativistic charged particle crossing an artificial periodic nano-scale multilayer structure in Lauer geometry in the general case of asymmetric refection in relation to inlet surface of the target is developed. Analytical expressions are derived for the spectral-angular distribution of PXR and diffracted transition radiation (DTR) based on two-wave approximation of dynamic scattering theory. It is shown that at fixed Bragg angle and path length of relativistic electron in target the radiation yield in a multilayer structure can considerably exceed the yield of the radiation in the crystal medium. It is also shown that the yields of PXR and DTR strongly depend on the angle between reflected layers and inlet surface of the multilayer target, *i.e.* on the reflection asymmetry. It is shown that the DTR contribution to the total yield of the radiation becomes determinant for high energy of incident electrons.

REFERENCES

[1] TER-MIKAELIAN M., *High-Energy Electromagnetic Process in Condensed Media* (Wiley, New York) 1972.
[2] PIESTRUP M. A., BOYERS D. G. and PINCUS C. I. *et al.*, *Phys. Rev. A*, **45** (1992) 1183.
[3] NASONOV N. N., KAPLIN V. V., UGLOV S. R., PIESTRUP M. A. and GARY C. K., *Phys. Rev.*, **68** (2003) 3604.
[4] GARIBIAN G. and YANG C., *J. Exp. Theor. Phys.*, **61** (1971) 930.
[5] BARYSHEVSKY V. and FERANCHUK I., *J. Exp. Theor. Phys.*, **61** (1971) 944.
[6] BARYSHEVSKY V. and FERANCHUK I., *J. Phys. (Paris)*, **44** (1983) 913.
[7] CATICHA A., *Phys. Rev. A*, **40** (1989) 4322.
[8] BAZYLEV V. and ZHEVAGO N., *Emission From Fast Particles Moving in a Medium and External Fields* (Nauka, Moscow) 1987.
[9] PINSKER Z., *Dynamic Scattering of X-rays in Crystals* (Springer, Berlin) 1984.
[10] BLAZHEVICH S. and NOSKOV A., *Nucl. Instrum. Methods Phys. Res. B*, **266** (2008) 3770.
[11] BLAZHEVICH S. and NOSKOV A., *Nucl. Instrum. Methods Phys. Res. B*, **266** (2008) 3777.
[12] BLAZHEVICH S. and NOSKOV A., *J. Exp. Theor. Phys.*, **136** (2009) 1043.